

Resonant acceleration and diffusion of outer zone electrons in an asymmetric geomagnetic field

Scot R. Elkington¹

Laboratory for Atmospheric and Space Physics, University of Colorado, Boulder, Colorado, USA

Mary K. Hudson

Department of Physics and Astronomy, Dartmouth College, Hanover, New Hampshire, USA

Anthony A. Chan

Department of Physics and Astronomy, Rice University, Houston, Texas, USA

Received 3 December 2001; revised 7 June 2002; accepted 8 August 2002; published 14 March 2003.

[1] The outer zone radiation belt consists of energetic electrons drifting in closed orbits encircling the Earth between ~ 3 and $7 R_E$. Electron fluxes in the outer belt show a strong correlation with solar and magnetospheric activity, generally increasing during geomagnetic storms with associated high solar wind speeds, and increasing in the presence of magnetospheric ULF waves in the Pc-5 frequency range. In this paper, we examine the influence of Pc-5 ULF waves on energetic electrons drifting in an asymmetric, compressed dipole and find that such particles may be efficiently accelerated through a drift-resonant interaction with the waves. We find that the efficiency of this acceleration increases with increasing magnetospheric distortion (such as may be attributed to increased solar wind pressure associated with high solar wind speeds) and with increasing ULF wave activity. A preponderance of ULF power in the dawn and dusk flanks is shown to be consistent with the proposed acceleration mechanism. Under a continuum of wave modes and frequencies, we find that the drift resonant acceleration process leads to additional modes of radial diffusion in the outer belts, with timescales that may be appropriate to those observed during geomagnetic storms. *INDEX TERMS:* 2720

Magnetospheric Physics: Energetic particles, trapped; 2730 Magnetospheric Physics: Magnetosphere—inner; 2788 Magnetospheric Physics: Storms and substorms; 2778 Magnetospheric Physics: Ring current; 2116 Interplanetary Physics: Energetic particles, planetary

Citation: Elkington, S. R., M. K. Hudson, and A. A. Chan, Resonant acceleration and diffusion of outer zone electrons in an asymmetric geomagnetic field, *J. Geophys. Res.*, 108(A3), 1116, doi:10.1029/2001JA009202, 2003.

1. Introduction

[2] The Van Allen radiation belts are composed of energetic ions and electrons, gradient-curvature drifting in orbits encircling the Earth. The energetic ions comprising the proton radiation belt are confined mainly to the inner regions of the magnetosphere, inside distances of perhaps 2–3 Earth radii (R_E) from the center of the Earth, and result primarily from the decay of neutrons freed by cosmic rays impinging on the upper atmosphere [Walt, 1996]. The electron radiation belts, on the other hand, divide themselves into two distinct regions: an inner zone belt, extending from a few hundred kilometers above the surface of the Earth to distances of 2–2.5 R_E , and an outer zone population of electrons, extending from $\sim 3 R_E$ to somewhere between 5 and 7 R_E . In the outer zone, external contribu-

tions to the geomagnetic field begin to significantly alter the field configuration from that of a simple dipole, with the solar wind compressing and increasing the magnetic field on the dayside, and ring and tail currents stretching and distorting the nightside magnetic field. The “slot region” between the inner and outer zones is kept largely free of trapped electrons through wave-particle interactions prevalent in this region [Kennel and Petschek, 1966]. The radiation belts as a whole are largely field-aligned structures, with outer zone electrons extending approximately $\pm 50^\circ$ from the geomagnetic equator.

[3] Inner zone populations are observed to be largely stable in time; however, electrons in the outer zone can show substantial variation on a variety of timescales. In particular, solar storms can have a profound effect on energetic electron fluxes observed in the outer zone. For example, in the sudden commencement phase of a storm, induced electric fields caused by the compression of the magnetosphere can impulsively inject solar and outer zone electrons into the inner regions of the magnetosphere. This was seen in the storm sudden commencement (SSC) of 24

¹Also at Space Science Institute, Boulder, Colorado, USA.

March 1991, which injected electrons inside the slot region and formed a new radiation belt over the course of a few minutes [Blake *et al.*, 1992; Li *et al.*, 1993]. In the initial portion of the main phase of a magnetic storm, on the other hand, energetic electron fluxes characteristically decrease in the outer zone. This decrease can be attributed to the “ D_{st} effect,” whereby decreases in the magnetic field strength resulting from the ring current buildup causes radiation belt particles to move radially outward through conservation of the third adiabatic invariant [Kim and Chan, 1997; Li *et al.*, 1997]. In the recovery phase of the storm, one might expect the radiation belts to increase to their prestorm levels as the D_{st} index increased toward zero. However, storm-time energetic electron fluxes are often observed to increase simultaneously throughout the outer zone by 1–2 orders of magnitude over prestorm levels, on timescales ranging from a few hours to 1–2 days [Baker *et al.*, 1994b, 1998b]. In a study of three storms showing substantial electron flux increases undertaken by McAdams and Reeves [2001], it was found that recovering D_{st} could only account for 10–20% of the poststorm electron flux increase. As the penetrating nature of the electron radiation can pose a considerable threat to human activities in space, there has been a particular interest in understanding the physics of these flux increases [Wrenn, 1995; Baker *et al.*, 1994a, 1998a].

[4] While the physics behind the outer zone flux variations, particularly the recovery phase increase of energetic electron fluxes, is not yet well understood, several intriguing correlations between solar and magnetospheric phenomena and the dynamics of the outer zone have been observed. Paulikas and Blake [1979], Baker *et al.* [1997], and Li *et al.* [1997] have all noted correlations between solar wind velocity and outer zone electron fluxes. Further, a strong correlation between ULF wave power in the Pc-5 frequency range (2–7 mHz [see Jacobs *et al.*, 1964]) and outer zone fluxes has been observed. For example, in a comparison of the 27 May 1996 magnetic cloud event with that of 10–11 January 1997, Baker *et al.* [1998b] found that large-amplitude oscillations in the Pc-5 frequency range were associated with the relativistic electron event of the 1997 storm, while the 1996 storm, which did not exhibit extensive Pc-5 activity, had no comparable increase in electron fluxes. Even more compelling, Rostoker *et al.* [1998] observed a strong correlation between outer zone fluxes and ULF activity over a 90 day period, with large increases in wave power preceding increases in geosynchronous electron fluxes by 1–2 days. Likewise, Mathie and Mann [2000a] studied a 6 month period in 1995 and found a strong association between geosynchronous electron fluxes and ULF power. Finally, confirming the link between solar wind speed, ULF wave activity, and energetic electron fluxes, O’Brien *et al.* [2001] used a cross correlation to determine which parameters in the solar wind and magnetosphere might most influence energetic electron fluxes. They found sustained solar wind speeds in excess of 450 km/s to be a strong external indicator of increasing magnetospheric electron fluxes, and long-duration Pc-5 activity during the recovery phase of a storm to be the best discriminator between those storms that produced relativistic electrons and those that did not.

[5] Ground observations suggest that Pc-5 ULF oscillations are most prevalent in the dawn sector of the magneto-

sphere [Anderson *et al.*, 1990; Ruohoniemi *et al.*, 1991; Glassmeier and Stellmacher, 2000], and have a higher occurrence rate during periods of high solar wind speed [Kokubun *et al.*, 1989; Engebretson *et al.*, 1998]. The source of wave power driving Pc-5 oscillations has been speculated to be either through Kelvin-Helmholtz waves generated by the flow of the solar wind past the magnetospheric boundary surface [Cahill and Winckler, 1992; Mann *et al.*, 1999], or through variations in the solar wind pressure propagating as wave energy into the magnetosphere [Lysak and Lee, 1992]. In a study examining phase velocities of magnetospheric ULF waves, Mathie and Mann [2000b] found that morning-sector waves during high speed solar wind events ($v_{sw} \simeq 500$ km/s) were likely driven by magnetopause flow instabilities, whereas during lower solar wind velocities observed ULF pulsations were likely a result of the impulsive action of the solar wind.

[6] A link between wave activity and particle dynamics is provided via radial diffusion theory. Here stochastic variations in the electric and magnetic fields guiding the trapped particle’s drift result in diffusion of particles across drift shells through violation of the third adiabatic invariant [Fälthammar, 1965, 1966, 1968; Cornwall, 1968; Schulz and Eviatar, 1969; Schulz and Lanzerotti, 1974]. If the first adiabatic invariant is conserved during this process, electrons will change energy as they move into regions of differing magnetic field strength. The spatial structure and energy spectrum of the radiation belts is consistent with radial diffusion [Lyons and Thorne, 1973]; however, timescales classically cited for radial diffusion processes are too slow to account for the storm time variations observed in the outer belts [Walt, 1996]. Li *et al.* [2001], on the other hand, found that they could accurately reproduce the time-history of geosynchronous electron fluxes using an ad hoc diffusion coefficient (based largely on solar wind velocity) to transport particles to geosynchronous from beyond 11 R_E .

[7] A number of other theories have been proposed to explain the connection between Pc-5 ULF waves and energetic electron dynamics. Liu *et al.* [1999] suggested that electron acceleration occurs as a result of magnetic pumping via pitch angle scattering and flux tube motion associated with ULF waves. Summers and Ma [2000] examined acceleration via a cyclotron interaction between trapped electrons and the compressional component of fast-mode ULF waves. Assuming a source of rapid pitch angle scattering to maintain an isotropic distribution, Summers and Ma [2000] predicted electron acceleration on timescales of a few hours.

[8] Using 3d, global MHD simulations of the magnetosphere driven by solar wind parameters measured by the WIND spacecraft at L_1 for the 10–11 January 1997 CME-magnetic cloud event, Hudson *et al.* [1999, 2000] modeled the evolution of relativistic electron fluxes in the equatorial plane using the MHD data as input to a guiding center test particle code. They proposed a drift-resonant acceleration mechanism resulting from ULF wave activity present in the simulations and the radial asymmetries seen in the outer zone magnetic field. This work was quantified by Elkington *et al.* [1999] for the case of toroidal-mode field line resonances. The purpose of this paper is to extend the work initiated by Elkington *et al.* [1999] to poloidal field line resonances and time-dependent convection electric fields,

and to show how such drift-resonant acceleration can lead to new modes of radial diffusion in the outer zone, with timescales commensurate with those often observed during geomagnetic storms.

2. Drift Resonant Acceleration

[9] We investigate the effects of ULF waves on energetic electron dynamics by tracking the guiding-center motion of equatorial particles moving under the influence of model electric and magnetic fields. Although these simulations lack off-equatorial dynamics, and are not capable of modeling those interactions which break the first adiabatic invariant, such simulations have shown themselves capable of capturing a broad range of physical processes and interactions relevant to radiation belt electrons [e.g., *Li et al.*, 1993, 1998; *Hudson et al.*, 1997, 2001; *Elkington et al.*, 2002].

[10] Here we use the same magnetic field model as that of *Elkington et al.* [1999], namely

$$B(r, \phi) = \frac{B_0 R_E^3}{r^3} + b_1(1 + b_2 \cos \phi). \quad (1)$$

The first term represents a dipole magnetic field of strength B_0 at the surface of the Earth, while the second term models the compression of the field resulting from solar wind dynamic pressure. Azimuthal angle ϕ is taken to be zero at local noon and increasing in a counter-clockwise sense, and constants b_1 and b_2 are selected based on measured magnetic field values. An equatorial particle drifting in such a field will drift along contours of constant magnetic field strength, characterized by a parameter

$$\mathcal{L} = \left(\frac{R_E^3}{r^3} + \frac{b_1 b_2 B_0}{\cos \phi} \right)^{-1/3}, \quad (2)$$

discussed further in Appendix A. \mathcal{L} is physically analogous to the third-adiabat conserving Roederer L , $L^* = -2\pi B_0/\Phi R_E$ [Roederer, 1970], where Φ is the magnetic flux enclosed in a drift path.

[11] The electric fields are modeled using

$$\mathbf{E}(r, \phi, t) = \mathbf{E}_0(r, \phi) + \sum_{m=0}^{\infty} \delta E_{rm} \sin(m\phi \pm \omega t + \xi_{rm}) \hat{\mathbf{r}} + \sum_{m=0}^{\infty} \delta E_{\phi m} \sin(m\phi \pm \omega t + \xi_{\phi m}) \hat{\boldsymbol{\phi}}, \quad (3)$$

where the first term represents any constant background magnetospheric convection fields, while the following terms are a superposition of global toroidal and poloidal field line resonances in the equatorial plane. Here m represents the azimuthal mode number of the ULF wave, ω the frequency, and δE_{rm} ($\delta E_{\phi m}$) and ξ_{rm} ($\xi_{\phi m}$) the amplitude and phase lag, respectively, of the toroidal (poloidal) mode m . Waves moving in the same direction as the eastward gradient drifting electrons will be referred to as propagating waves; those moving in the opposite direction are referred to as counterpropagating. Note that for $m = 1$ and a standing wave consisting of both propagating and counterpropagating waves of equal amplitude δE and zero phase ξ , the time-dependent part of equation (3) can also describe a time varying, dawn-dusk convection electric field varying with amplitude $2\delta E$ and frequency ω .

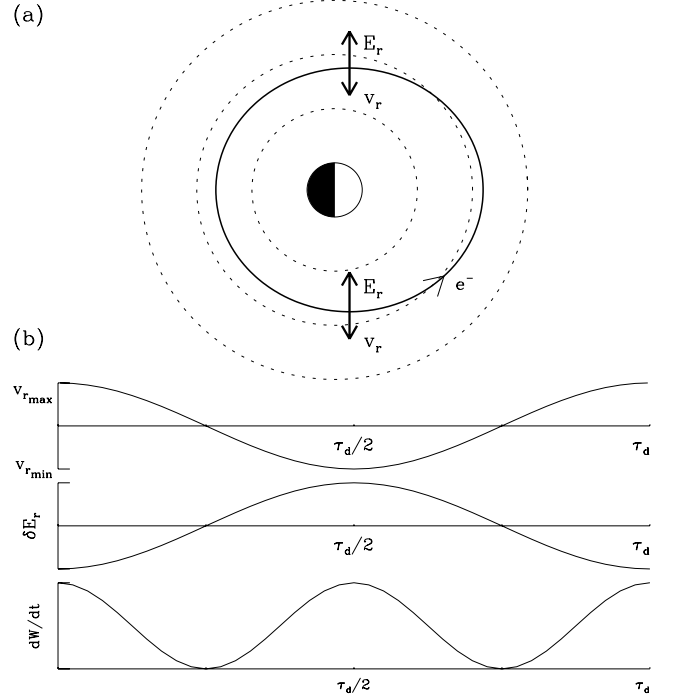


Figure 1. (a) Sketch of an electron drift path in a compressed dipole, with electric fields indicated for a toroidal oscillation in an $m = 2$ mode. (b) Radial drift velocity, radial electric field, and rate of change of energy seen by a resonant particle starting at local dawn.

[12] The energy gained by an electron moving adiabatically in an electric field is given by

$$\frac{dW}{dt} = q\mathbf{E} \cdot \mathbf{v}_d + M \frac{\partial B}{\partial t}, \quad (4)$$

where \mathbf{v}_d is the total particle drift velocity [Northrop, 1963]. The second term in equation (4) is zero in the equatorial plane for the fundamental toroidal mode studied by *Elkington et al.* [1999], since the magnetic perturbation δB_ϕ has a node at the equator. The dominant radial component of the fundamental poloidal mode, δB_r , also has a node at the equator, while the compressional δB_\parallel component is smaller in amplitude for low kinetic to magnetic pressure ratio (plasma beta) characteristic of the outer zone electron region; thus the second term in equation (4) is neglected in this study.

2.1. Compressed Dipole Resonance: Toroidal Mode

[13] The effect of a global, monochromatic toroidal-mode field line resonance on an energetic electron was discussed in some detail by *Elkington et al.* [1999]; a brief review will be given here. The proposed acceleration mechanism is illustrated in Figure 1. Here an equatorially mirroring electron in a compressed dipole interacts with a global $m = 2$ toroidal-mode wave of frequency ω . An electron starting at dusk and moving with a drift frequency $\omega_d = \omega$ would first see a positive radial electric field while undergoing negative radial motion, and half a drift period later a negative electric field while moving radially outward. As indicated in Figure 1b, the resulting product $E_r dr$ is therefore negative over the orbit of the electron, leading to a net

energy increase via equation (4). For arbitrary m , the resonance condition for drift-resonant acceleration is given by (Appendix B)

$$\omega - (m \pm 1)\omega_d = 0. \quad (5)$$

[14] To verify the resonant nature of this acceleration, particles of different initial energies (and hence different drift frequencies) can be started in a single specified mode, and maximum energy gain recorded. An example is shown in Figure 2a for a 4 mHz, 3 mV/m field in an $m = 2$ mode, with no convection electric field. All electrons are started at local dusk; those with energies near \mathcal{E}_1 ($\omega_d = \omega$) see the greatest increase in energy. Also, consistent with equation (5), a second peak is clearly evident where $\omega_d = \omega/3$, at energy \mathcal{E}_3 . The range of electron energies over which an electron will experience resonant acceleration was given by *Elkington et al.* [1999], and is developed in Appendix B.

[15] Phase space plots of the particle motion provide a useful way of examining the behavior of a driven system [e.g., *Lichtenberg and Lieberman*, 1983]. Figure 2b shows a Poincaré plot consisting of the particle energy and azimuthal position recorded at increments of one wave period; the resulting plot shows the expected resonant island centered at $\mathcal{E}_1 \sim 3.14$ MeV, and three smaller islands at \mathcal{E}_3 around 850 keV, consistent with equations (5) and (B6). The dropout in energy gain seen at \mathcal{E}_1 in panel (a) is a result of the saddle point at $\phi_0 = 270$ degrees in panel (b). For the electrons and fields used to generate panels (a) and (b), and a radial displacement $\delta r = 0.23 R_E$ from equation (A3), the resonant width predicted by equation (B6) is ~ 0.17 MeV, in good agreement with the maximum energy gain in Figure 2a and primary island width in Figure 2b.

[16] The effect of a constant, dawn-dusk convection electric field $E_0 \hat{y}$ on an electron's phase plane dynamics is depicted in Figure 2c for a single particle beginning at a point outside the resonant separatrix. The uniform convection field transforms the primary resonant center in the reduced phase space of panel (b) into a feature resembling a stable attractor. An important implication of this result is that particles may be adiabatically accelerated from energies outside the resonance described in equations (5) and (B6). In principle it is possible to adiabatically accelerate electrons with 10–100 keV energies at the magnetopause to MeV energies in the inner magnetosphere, using drift-resonant acceleration and a strong convection electric field. For example, an electron with an initial energy of 80 keV at $10 R_E$ at local noon would have an energy around 200 keV at geosynchronous, and exceeding 1.1 MeV at $3 R_E$.

[17] A second implication of the effect of the convection field is that it is possible to accelerate particles in bulk using resonance with toroidal waves. That is, without the effect of the convection fields, particles on one side of the resonance would gain energy while particles on the other side of the resonance would lose energy, resulting in a bulk acceleration limited to that arising from energy asymmetries in the resonant island. The addition of the convection electric field makes it possible to accelerate particles regardless of their initial phase.

2.2. Compressed Dipole Resonance: Poloidal Mode

[18] The nature of the resonant interaction of an electron with a poloidal mode oscillation is indicated in Figure 3.

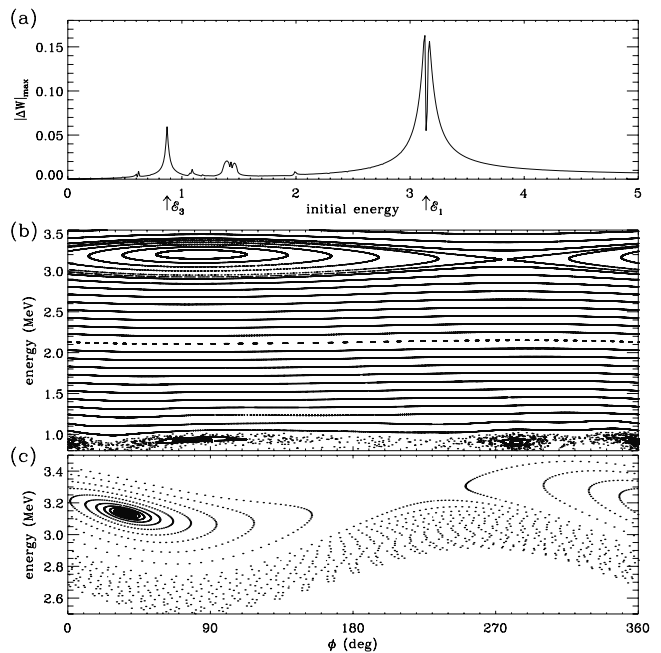


Figure 2. (a) Energy gained by electrons with different initial energies in a 3 mV/m, $m = 2$ toroidal electric field oscillating at 4 mHz, each particle beginning at $5.0 R_E$ at dusk local time. \mathcal{E}_1 and \mathcal{E}_3 indicate the energies of electrons with $\omega_d = \omega$ and $\omega_d = \omega/3$, respectively. (b) Poincaré map showing the phase plane dynamics of particles with uniform first adiabatic invariant, moving in the same purely toroidal-mode fields as (a). (c) Poincaré map of a single particle starting at local dusk at 2.5 MeV moving with the same first adiabatic invariant and toroidal fields as above, with the addition of a uniform dawn-dusk convection electric field of 5 mV/m.

Here a resonant electron will see a positive E_ϕ in the midnight sector and a negative E_ϕ in the noon sector, where the sign of E_ϕ is determined in the usual right-hand sense. The change in energy over the course of the electron's motion is again determined by equation (4), with the second term neglected for low plasma beta. In a purely dipolar field, one would expect the energy gained at local midnight, where v_d and E_ϕ are antiparallel, to exactly balance the energy lost at local noon, where v_d and E_ϕ are parallel, resulting in no net increase in the electron's energy over the course of its motion unless pitch angle scattering or some other first invariant-breaking mechanism is invoked [e.g., *Liu et al.*, 1999; *Summers and Ma*, 2000]. However, in a distorted dipole, where the azimuthal drift velocity is given by equation (A7), the energy gained in the midnight sector will exceed that lost in the noon sector, resulting in a net energy increase over the course of a drift orbit. This mechanism leads to the same $\omega = (m \pm 1)\omega_d$ resonance condition as found in the toroidal situation.

[19] The Poincaré plots corresponding to a poloidally resonant electron are indicated in Figure 4, for the same particle first adiabatic invariant and the same field frequency, magnitude, and mode structure as used in Figure 2. The primary resonant center shows symmetry about the noon-midnight line, as might be expected from Figure 3.

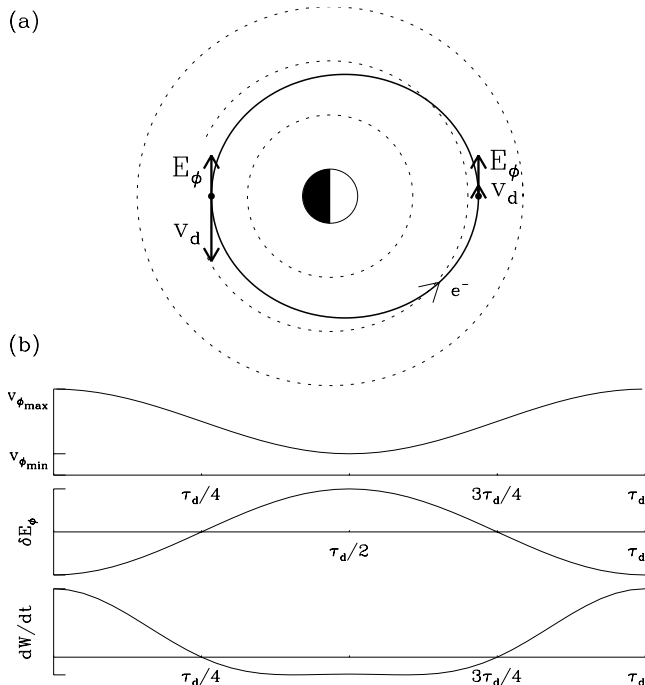


Figure 3. (a) Sketch of an electron drift path in a compressed dipole, with electric fields seen by an electron resonant with poloidal-mode oscillations indicated at noon and midnight. The differing drift velocities at noon and midnight are qualitatively indicated by the vector length v_d at each location. (b) Azimuthal drift velocity, electric field, and rate of change of energy seen by a poloidally resonant particle starting at local midnight.

[20] The effects of a convection electric field is indicated in Figure 4b, where three particles have been started with different initial conditions and allowed to evolve for identical periods of time. In contrast to the toroidal mode, convection fields have the effect of changing the resonant islands of (Figure 4a) into *unstable* centers. Those electrons beginning at locations above the resonant separatrix gain energy, while those beginning below the separatrix tend to lose energy. For those electrons with initial locations inside the resonant island, the question of whether or not they ultimately gain or lose energy depends sensitively on both initial energy and azimuthal location.

[21] While the poloidal mode is capable of accelerating particles, equation (4) and the fact that the drift velocity decreases with the relativistic correction factor γ imply that the electrons above the separatrix in Figure 4b will gain energy more slowly than electrons below the separatrix will lose energy. For electron distributions exhibiting a steep power law in energy \mathcal{W} , such as is commonly observed in the outer radiation belts, this asymmetry should lead to a net decrease in energy of the electrons as a whole. This result suggests that a necessary condition for bulk energization under the influence of a single-frequency wave is that there be more power in the toroidal mode than the poloidal mode. This suggestion is consistent with MHD simulations of the January 1997 magnetic storm [Hudson *et al.*, 2000], while analysis of magnetometer measurements from the Equator-S spacecraft for the March 1998 storm [Nakamura *et al.*, 2002] show that both polarizations are present over a range

of frequencies (0.5–10 mHz) on the dawn side of the magnetosphere between $L = 5$ –10, near the equatorial plane, where the measurements were made. Statistical studies of occurrence properties will be described later.

2.3. Symmetric Resonance

[22] While the convection electric field has an important and interesting effect on both toroidal and poloidal field line resonances, the relative field orientations and axes of symmetry of Figures 1 and 3 suggest that ULF variations in the global dawn-dusk convection electric field itself might serve as an efficient acceleration mechanism in the absence of either toroidal or poloidal oscillations. The acceleration mechanism is indicated in Figure 5, depicting an electron moving in a symmetric (dipole) magnetic field under the influence of a dawn-dusk convection electric field varying with frequency $\omega = m\omega_d$. The phase-plane dynamics corresponding to this case are indicated in Figure 6, where 5 mV/m fields with superposed 4 mHz, 3 mV/m oscillations interact with electrons of the same first adiabatic invariant as in Figures 2 and 4. As can be seen by comparing the resonant interaction width of the oscillating convection electric field with those of the toroidal and poloidal modes, a coherent time-dependent convection electric field can potentially provide much greater energization for the same amplitude of oscillation.

[23] A source of ULF power in the convection electric field might arise via direct coupling from the solar wind. Dungey [1961] showed that polar convection, the ionospheric manifestation of magnetospheric convection, could be explained by invoking magnetic reconnection with the interplanetary magnetic field at the magnetopause. Subsequent work has shown that magnetospheric convection

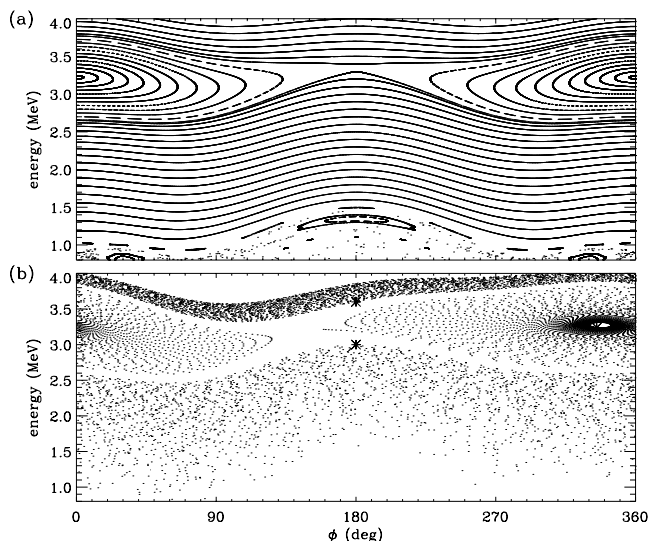


Figure 4. (a) Poincaré map showing the phase plane dynamics of particles with uniform first adiabatic invariant, moving in the same 3 mV/m, 4 mHz, $m = 2$ fields as Figure 2, but in a poloidal mode. (b) Poincaré map showing particle dynamics with the same first adiabatic invariant and fields as (a), but with the addition of a convection electric field of 5 mV/m. Asterisks indicate the initial azimuth and energy of individual particles.

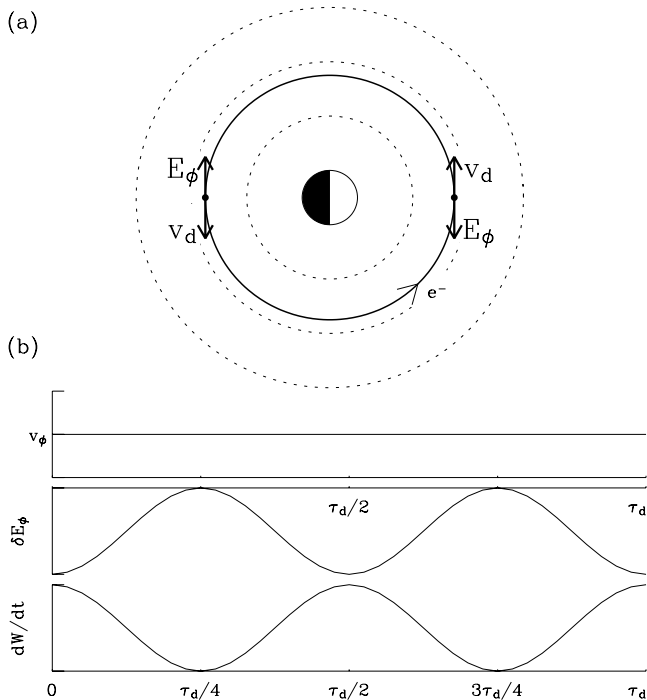


Figure 5. (a) Sketch of an electron drift path in a symmetric dipole, with electric fields indicated for an $m = 1$ standing oscillation corresponding to a time-varying dawn-dusk convection electric field. (b) Drift velocity, azimuthal electric field, and rate of change of energy seen by a resonant electron.

tracks time variations in the IMF [Birmingham, 1969; Nishida and Maezawa, 1971; Saunders et al., 1992], and possibly at \sim minute timescales [Ridley et al., 1997, 1998; Ruohoniemi and Greenwald, 1998]. The solar wind coupling parameter suggested by Perreault and Akasofu [1978], of the form

$$\varepsilon = v_{sw} B_{sw}^2 \ell_0^2 \sin^4(\theta/2), \quad (6)$$

estimates the rate at which energy is transmitted from the Poynting flux in the solar wind into the magnetosphere via magnetic reconnection at the magnetopause. Here v_{sw} is the solar wind velocity, B_{sw} the magnitude of the IMF, θ the “clock angle” between the IMF and the Earth’s magnetic dipole, and $\ell_0 = 7 R_E$. Variations in ε , therefore, might be expected to translate directly into variations in the convection electric field.

[24] Time-dependent convection electric fields at a single frequency, in contrast to toroidal and poloidal oscillations, are not capable of accelerating electrons in bulk as the resonant centers show no stable or unstable characteristics. That is, for electrons evenly distributed in azimuth on a shell of constant L , one would expect that for every electron in phase with the wave and gaining energy there would be a corresponding electron out of phase with the wave and losing energy, resulting in no net increase in energy when integrated over all electrons in that shell. However, in the case of multiple ULF wave frequencies, the greatly increased resonant interaction width results in the potential

for very efficient acceleration through the resonant diffusion process, as outlined in section 4.

3. Local Time and Propagation Effects

[25] In the preceding examples, the test particles interacted with a single propagating mode acting globally over the course of the electron orbit. However, statistical studies by ground-based magnetometers of Pc-5 waves indicate that the preponderance of ULF wave activity occurs on the flanks, with perhaps more activity in the dawn sector [Anderson et al., 1990; Ruohoniemi et al., 1991]. Further, if the ULF wave activity is a result of flow instabilities along the flanks [Cahill and Winckler, 1992; Mann et al., 1999; Mathie and Mann, 2000b], one would expect the wave power to be directed generally tailward, i.e., propagating eastward in the dusk sector and westward in the dawn sector. How would electron acceleration be affected in each case?

[26] The answer is indicated in Figure 7, where we schematically show the drift velocity of an energetic electron, along with the electric fields seen by the particle for eastward propagating (dotted line) and westward propagating (dashed line) waves. In the case of a global westward propagating wave, opposite the direction of electron drift, the net energization seen over the course of the orbit clearly integrates to zero (panel c). However, if the wave activity is assumed to occur only along the flanks (solid lines), we see that we can in fact energize the particle, through interaction with the eastward propagating mode at dusk and westward propagating mode at dawn.

[27] Glassmeier and Stellmacher [2000] note that satellite observations show Pc-5 activity to be symmetrically distributed, and suggest that the asymmetry perceived by ground-based measurements is a result of ionospheric screening. However, global occurrence of ULF waves does not seem to be a requisite factor in the drift-resonant acceleration of electrons, and, in the case of westward

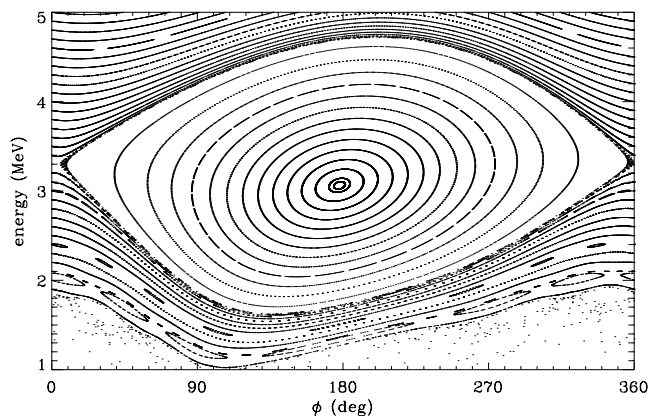


Figure 6. Poincaré map showing the phase plane dynamics of particles with the same first adiabatic invariant as in Figures 2 and 4, but under the influence of a standing $m = 1$ oscillation corresponding to a time-dependent convection electric field. The amplitude of the convective field is 5 mV/m with superposed 4 mHz oscillations of 3 mV/m.

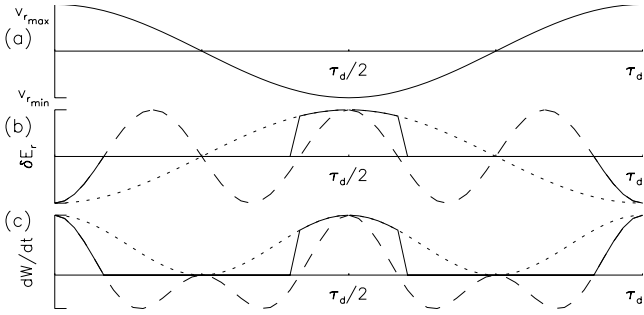


Figure 7. Electron dynamics for an electron initially at dawn moving in a compressed dipole under the influence of eastward propagating (dotted line) and westward propagating electric fields (dashed line). The solid lines in panels (b) and (c) indicate the electric field and energy change for an electron seeing only eastward propagating waves in the dusk sector and westward propagating waves in the dawn sector, corresponding to tailward-directed Kelvin-Helmholtz waves.

propagating ULF waves, a local time asymmetry is in fact required for energization to occur.

4. Multiple Frequencies: Radial Diffusion

[28] The previous sections dealt with the dynamics of electrons moving under the influence of a monochromatic oscillation in a single mode. While there are instances where this is observed to be largely the case, as in the period around 1100 UT on 10 January 1997 [Hudson *et al.*, 1999], one would, in general, expect a superposition of global modes and frequencies to exist simultaneously. This section deals with the effects of multiple ULF frequencies on global electron dynamics.

4.1. Radial Diffusion in a Compressed Dipole

[29] Figure 8 shows the effect of two toroidal-mode waves of differing frequencies on the phase-plane dynamics of electrons conserving their first invariant. As indicated in (Figure 8a), when the boundaries of the resonant islands begin to overlap, the motion of the electrons becomes chaotic in phase space. This leads to stochastic diffusion in energy, and, through conservation of the first adiabatic invariant, diffusion in \mathcal{L} . (Figure 8b) shows the fully stochastic motion of electrons moving under the influence of two waves with a slightly smaller frequency separation than in (Figure 8a). According to the Chirikov overlap criterion [Chirikov, 1979], this transition to fully diffusive motion will occur when the sum of the half-widths (B6) of the two islands, calculated independently, just equals the distance between the resonances. However, numerical results indicate that the onset of stochastic motion will actually occur when the ratio of the sum of the island widths to their separation distance is approximately 2/3, due to the interaction of higher-order resonances [Lichtenberg and Lieberman, 1983].

[30] The diffusion coefficient, D_{WW} , corresponding to the particle diffusion in energy space, will here be defined by

$$D_{WW} \equiv \frac{\langle (\Delta W)^2 \rangle}{2\tau}, \quad (7)$$

where the term in angle brackets denotes the ensemble average deviation in energy taken over a time $\tau \gg T_d$, the particle drift period [see, e.g., Schulz and Lanzerotti, 1974]. The functional dependence of this diffusion can be calculated as follows. For a continuum of purely toroidal waves, an approximate form for the energy diffusion can be obtained by using the maximum possible energy gained over the course of a drift orbit as a step-size for a random walk in energy space. That is,

$$D_{WW}^{(t)} \sim \frac{e^2 \delta E_r^2 \delta r^2}{2T_d}, \quad (8)$$

where the superscript “(t)” signifies resonant diffusion due to interaction with toroidal-mode waves. Using the radial displacement δr given by equation (A4) for an asymmetric (compressed) dipole background field, and the unperturbed drift period, given by equation (A6) with $b_1, b_2 = 0$, we find a functional form for D_{WW} at constant first adiabatic invariant, M of

$$D_{WW}^{(t)} \sim \frac{2}{3\pi} \frac{eMc}{\gamma} \mathcal{L}^6 \left(\frac{b_1 b_2}{B_0} \right)^2 P(\omega_{m\pm 1}), \quad (9)$$

where $P(\omega_{m\pm 1})$ is the power in the electric field spectrum in the range of frequencies interacting with the “ $m \pm 1$ ” drift resonance of the particle in question. It should be noted that, in addition to the radial dependence \mathcal{L}^6 , the rate of diffusion increases with the square of the radial distortion, indicated by the $b_1 b_2 / B_0$ term, and exhibits an energy dependence through the relativistic correction factor γ . At constant M , the rate of radial diffusion will scale directly with the rate of energy diffusion. The corresponding radial diffusion coefficient can be found by recalling that, in the relativistic

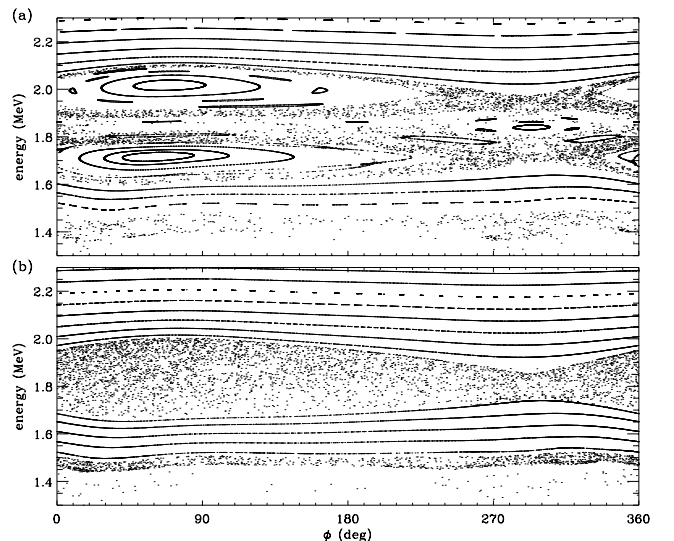


Figure 8. (a) Phase-plane dynamics of 0.0345 MeV/nT electrons under the influence of two toroidal-mode waves, at 1.85 and 2.15 mHz, showing the onset of diffusive behavior as the resonant islands begin to overlap. (b) Phase-plane dynamics of the same electrons under the influence of 1.90 and 2.10 mHz waves, showing fully diffusive behavior in the resonant overlap region.

limit, $W \sim \mathcal{L}^{-3/2}$ [e.g., *Hudson et al.*, 1997], so that $dW \sim \mathcal{L}^{-5/2}d\mathcal{L}$, and

$$D_{LL}^{(t)} \equiv \frac{\langle(\Delta\mathcal{L})^2\rangle}{2\tau} \propto \frac{M}{\gamma} \mathcal{L}^{11} \left(\frac{b_1 b_2}{B_0}\right)^2 P(\omega_{m\pm 1}). \quad (10)$$

Thus, for P independent of \mathcal{L} , the rate of radial diffusion due to interaction with a spectrum of global, toroidal-mode ULF waves might be expected to show an \mathcal{L}^{11} dependence.

[31] The functional form of the resonant diffusion due to interaction with a spectrum of poloidal-mode waves in an asymmetric (compressed) dipole background field may be found in a similar fashion. From equation (4), we find an approximate expression for the maximum energy gain over a drift orbit of $\Delta W \simeq 2e\delta E_\phi \delta v T_d$, where δv is given by equation (A10). The energy diffusion (7) can thus be written

$$D_{WW}^{(p)} \sim \frac{128\pi}{3} \frac{eMc}{\gamma} \mathcal{L}^6 \left(\frac{b_1 b_2}{B_0}\right)^2 P(\omega_{m\pm 1}), \quad (11)$$

and the radial diffusion due to poloidal interaction is likewise

$$D_{LL}^{(p)} \propto \frac{M}{\gamma} \mathcal{L}^{11} \left(\frac{b_1 b_2}{B_0}\right)^2 P(\omega_{m\pm 1}). \quad (12)$$

We see that asymmetric diffusion due to the poloidal mode exhibits the same functional form as that due to the toroidal mode. However, comparison of equations (9) and (11) suggests that poloidal diffusion is likely to be substantially more efficient than toroidal diffusion because of the larger coefficient in (11).

[32] Previous theoretical treatments of trapped particle diffusion have assumed stochastic variations in either the magnetic or electric field, occurring on drift-period timescales, which violate the third adiabatic invariant Φ while conserving M and J . These treatments can be broadly categorized as either magnetic diffusion [*Fälthammar*, 1968; *Schulz and Viatar*, 1969] or electric diffusion [*Cornwall*, 1968; *Fälthammar*, 1965, 1966, 1968; *Birmingham*, 1969]. A complete theoretical treatment of each is outlined by *Schulz and Lanzerotti* [1974]. The magnetic diffusion coefficient, $D_{LL}^{(m)}$, is usually written for equatorial electrons as

$$D_{LL}^{(m)} = 2\omega_d^2 \left(\frac{5B_2}{21B_1B_0}\right)^2 L^{10} \left(\frac{R_E}{R_S}\right)^2 P_{B_z}(\omega_d), \quad (13)$$

where B_1 , B_2 , and R_S are coefficients used in the Mead magnetospheric model [*Mead*, 1964] assumed in this analysis, and P_{B_z} is the spectral density of magnetic disturbances at the drift frequency of the trapped particles. The energy dependence of the diffusion coefficient is contained explicitly in the ω_d term and implicitly in the assumed form of $P_{B_z}(\omega_d)$. If one assumes the disturbance rises quickly and decays slowly on the timescale of the drift of the particle, then $P_{B_z} \propto \omega_d^{-2}$, so that equation (13) is independent of energy [*Schulz and Lanzerotti*, 1974]. Under this assumption, the diffusion coefficient reduces to the simple form $D_{LL}^{(m)} = D_0^{(m)} L^{10}$.

[33] A similar analysis corresponding to electric field fluctuations results in a diffusion coefficient of the form

$$D_{LL}^{(e)} = 2 \left(\frac{c}{4R_E B_0}\right)^2 L^6 \sum_m m^2 P_{m,\epsilon}(m\omega_d), \quad (14)$$

where here the energy dependence arises in the assumed or measured form of P_ϵ , the spectral power of electric field fluctuations at the drift frequency ω_d . It should be noted that the analysis resulting in this form assumes a symmetric dipole magnetic field and only considers the effect of azimuthal electric fields. Under these conditions, we refer to the diffusion as the symmetric mode of diffusion. For the special case of $m = 1$, corresponding to the convection electric field variations discussed in section 2.3, the resulting diffusion coefficient is

$$D_{LL}^{(e)} = 2 \left(\frac{c}{4R_E B_0}\right)^2 L^6 P_\epsilon(\omega_d), \quad (15)$$

This is the same result arrived at by *Cornwall* [1968], *Fälthammar* [1968], and *Birmingham* [1969], and other early researchers considering diffusion of trapped energetic particles resulting from convection electric field variations. For the special case of electric field impulses that are again assumed to rise quickly with amplitude ΔE and decay exponentially with e-folding time $\tau \gg 2\pi/\omega_d$, the spectral power falls as ω_d^{-2} and equation (15) takes the form

$$D_{LL}^{(e)} = 4\omega_d^2 \left(\frac{eR_E}{24B_0}\right)^2 L^{10} \left(\frac{\gamma}{M}\right)^2 \frac{(\tau^2/T) \Sigma(\Delta E)^2}{1 + \omega_d^2 \tau^2} \quad (16)$$

where $\Sigma(\Delta E)^2$ is the sum of the squares of all sudden electric field fluctuations occurring in a time interval $T \gg \tau$ [*Schulz and Lanzerotti*, 1974].

4.2. Empirical Determination of D_{LL}

[34] Given the variety of forms exhibited by equations (13)–(16) and the range of assumptions involved in each form, there has been considerable effort to determine diffusion rates based on observational evidence, using a number of different techniques. A summary of a few of these results is indicated in Table 1; more extensive compilations can be found in the studies by *Lanzerotti et al.* [1970], *Tomassian et al.* [1972], *Holzworth and Mozer* [1979], and *Riley and Wolf* [1992], and elsewhere. Two of the works listed in the table, *Lanzerotti and Morgan* [1973] and *Holzworth and Mozer* [1979], assumed that diffusion rates were correctly given by equation (13) or (15) and used measured magnetic and electric field spectra to arrive at the relevant diffusion coefficients. The remainder of those listed in the table arrived at diffusion rates without an assumed L -dependence.

[35] The characteristic timescales exhibited in Table 1 range from ~ 1 day at $L = 6$ to several years for electrons in the inner belt. Except in the case of *Lanzerotti and Morgan* [1973], who found that the diffusion coefficient at $L = 4$ could vary by orders of magnitude with magnetic activity, the observations used in these analyses were generally made during quiet geomagnetic periods. Radial diffusion calculations carried out by *Selesnick and Blake* [2000] indicate

Table 1. Examples of Empirically Determined Radial Diffusion Coefficients

D_{LL} , day ⁻¹	L	W or M Range	Reference
2.0×10^{-7}	$L = 1.20$	$W > 1.6$ MeV	<i>Newkirk and Walt</i> [1968a]
4.0×10^{-6}	$L = 1.16$		
$10^{-8}L^{(10 \pm 1)a}$	$1.76 \leq L \leq 5.0$	$W > 1.6$ MeV	<i>Newkirk and Walt</i> [1968b]
$4-8 \times 10^{-10}L^{10 a}$	$3.0 \leq L \leq 5.0$	$W > 5$ MeV	<i>Lanzerotti et al.</i> [1970]
$2.7 \times 10^{-5}M^{-5}L^{7.9}$	$1.7 \leq L \leq 2.6$	13.3–27.4 MeV/G	<i>Tomassian et al.</i> [1972]
$10^{(0.75K_{FR}-10.2)b}$	$L = 4$	350–750 MeV/G	<i>Lanzerotti and Morgan</i> [1973]
$(2.23 \pm 0.67)\omega_d^{-1.1 \pm 0.15c}$	$L = 6.0$	50 keV–1.2 MeV	<i>Holzworth and Mozer</i> [1979]
$\sim 2-5.0$	$L = 5.3, L = 6.1$	100 keV–1.6 MeV	<i>Chiu et al.</i> [1988]
$2.1 \times 10^{-3}(\frac{L}{4})^{11.7 \pm 1.3}$	$3.0 \leq L \leq 6.0$	3–8 MeV	<i>Selesnick et al.</i> [1997]

^a D_0 based on an assumed L^{10} radial dependence.

^bBased on equation (13) and measured magnetic power spectrum; $K_{FR} \equiv$ Fredricksburg magnetic index [see also *Brautigam and Albert*, 2000].

^cBased on equation (15) and measured electric power spectrum; ω_d is expressed as h⁻¹.

that the diffusion coefficient can vary by at least a factor of 5 during disturbed geomagnetic conditions, suggesting that observed diffusive timescales at $L = 6$ can be as low as a few hours during storms.

[36] Two of the works listed in Table 1, *Newkirk and Walt* [1968b] and *Selesnick et al.* [1997], made an attempt to determine the radial dependence of outer zone diffusion coefficients based on particle measurements. The approach used by *Selesnick et al.* [1997], for example, examined electron dynamics over a 3-month period in 1996. Assuming a radial diffusion coefficient of form $D_{LL} = D_0(L/4)^n$ and a characteristic particle lifetime of form $\tau = \tau_0(L/4)^{-m}$, they were able to fit observations from three clear electron injections to a time-dependent radial diffusion equation with losses [*Schulz and Lanzerotti*, 1974] and deduce a radial diffusion coefficient varying as $L^{(11.7 \pm 1.3)}$, where the error bars were based on statistical rather than systematic considerations. *Newkirk and Walt* [1968b] similarly found a radial diffusion coefficient of $L^{(10 \pm 1)}$. The L^{11} dependence of diffusion in a compressed dipole indicated by equations (10) and (12) is consistent with each of these observations.

4.3. Characteristic Timescales

[37] (Figures 9a–9c) shows the relative effectiveness of the $\omega = m\omega_d$ and $(m-1)\omega_d$ or $(m+1)\omega_d$ forms of diffusion for azimuthal electric field fluctuations. In each case, 360 particles were distributed evenly in azimuth at a constant $\mathcal{L}_0 = 6.6$, and with an initial energy of $W_0 = 1$ MeV. They were then allowed to interact with global $m = 2$ oscillations in a range of frequencies designed to excite one of the three resonant modes, $\omega = (m-1)\omega_d$, $\omega = m\omega_d$, or $\omega = (m+1)\omega_d$, and the position and energy was recorded as a function of time. Here a symmetric magnetic field of dipole strength $B_0 = 27,500$ nT was used, and the parameters b_1 and b_2 were selected based on the noon and midnight field strengths at $6.6 R_E$ predicted by the *Tsyganenko and Stern* [1996] magnetic field model for magnetospheric conditions corresponding to the recovery phase of the 24–26 September 1998 magnetic storm. The simulation domain was selected to be $\mathcal{L} = \mathcal{L}_0 \pm 1$; those particles drifting beyond this domain were removed from the simulation. The range of frequencies used in each case were picked to excite the chosen resonant mode over the entire computational domain, without frequency components capable of exciting another resonance for any electron still within the computational domain. The frequency spectrum was chosen to be a flat profile of $\delta E_{r,\phi} = 0.1$ mV/m at frequency intervals of

0.1 mHz, for a constant power spectral density (PSD) of $P = \delta E^2/2\delta f = 5 \times 10^{-5}$ V²m⁻²Hz⁻¹, on the order of that commonly seen in MHD simulations of the storm-time magnetosphere [*Hudson et al.*, 2000]. The corresponding RMS wave amplitude exciting each individual mode, $E_{RMS} = \sqrt{P\Delta f}$, is about 0.3 mV/m over each 2 mHz interval, and 0.56 mV/m over the 0.5–6.7 mHz frequency interval. This is consistent with the electric field RMS wave amplitudes observed during moderately disturbed geomagnetic conditions [*Lyons and Thorne*, 1973; *Lyons and Schulz*, 1989; *Brautigam and Albert*, 2000].

[38] In the left-hand column of Figure 9, the mean square deviation $\langle (\mathcal{L} - \mathcal{L}_0)^2 \rangle$ was plotted as a function of time for each resonant mode. A linear least squares fit was applied to the time series of particle spread, and the slope of the fit line was used to calculate the diffusion coefficient via the corresponding equation (10) for the poloidal mode, $D_{LL}^{(p)} \equiv \langle (\Delta \mathcal{L})^2 \rangle / 2\tau$. In the right-hand column the particles were sorted and binned by $|\mathcal{L} - \mathcal{L}_0|$ after one hour of simulation time. A gaussian was fit to the resulting distribution, and a second numerical diffusion coefficient was calculated based on the half-maximum width of the gaussian fit.

[39] Panel (a) of Figure 9 shows the diffusion of particles moving under the influence of purely azimuthal electric fields in the compressed dipole field representative of the assumptions leading to equation (12) for the $(m-1)$ mode. For particles beginning at $\mathcal{L}_0 = 6$ and $W_0 = 1$ MeV in the specified fields, and adiabatically interacting with a global $m = 2$ mode within the simulation domain, the range of frequencies between 0.5 and 2.5 mHz will excite the $(m-1)$ mode. The diffusion coefficient calculated in this case is $D_{LL} \sim 7.5 \times 10^{-3}$ h⁻¹, corresponding to a diffusion timescale $\tau_{LL} \sim 134$ hours, on the order of 5–6 days.

[40] In panel (b) we show the diffusion corresponding to the $\omega = m\omega_d$ resonant mode, as might be found from equation (14). Here the range of frequencies chosen was between 2.5 and 4.5 mHz. We find an increased rate of radial transport over the $(m-1)$ mode, with diffusion timescales on the order of 46 h.

[41] Panel (c) of Figure 9 shows the $(m+1)$ diffusion mode, with corresponding wave frequencies between 4.7 and 6.7 mHz. The diffusion rates here are comparable to those of the symmetric mode, panel (b), on the order of two days.

[42] Finally, in panel (d), we allow the particles to interact with waves in the frequency range 0.5–6.7 mHz. This range

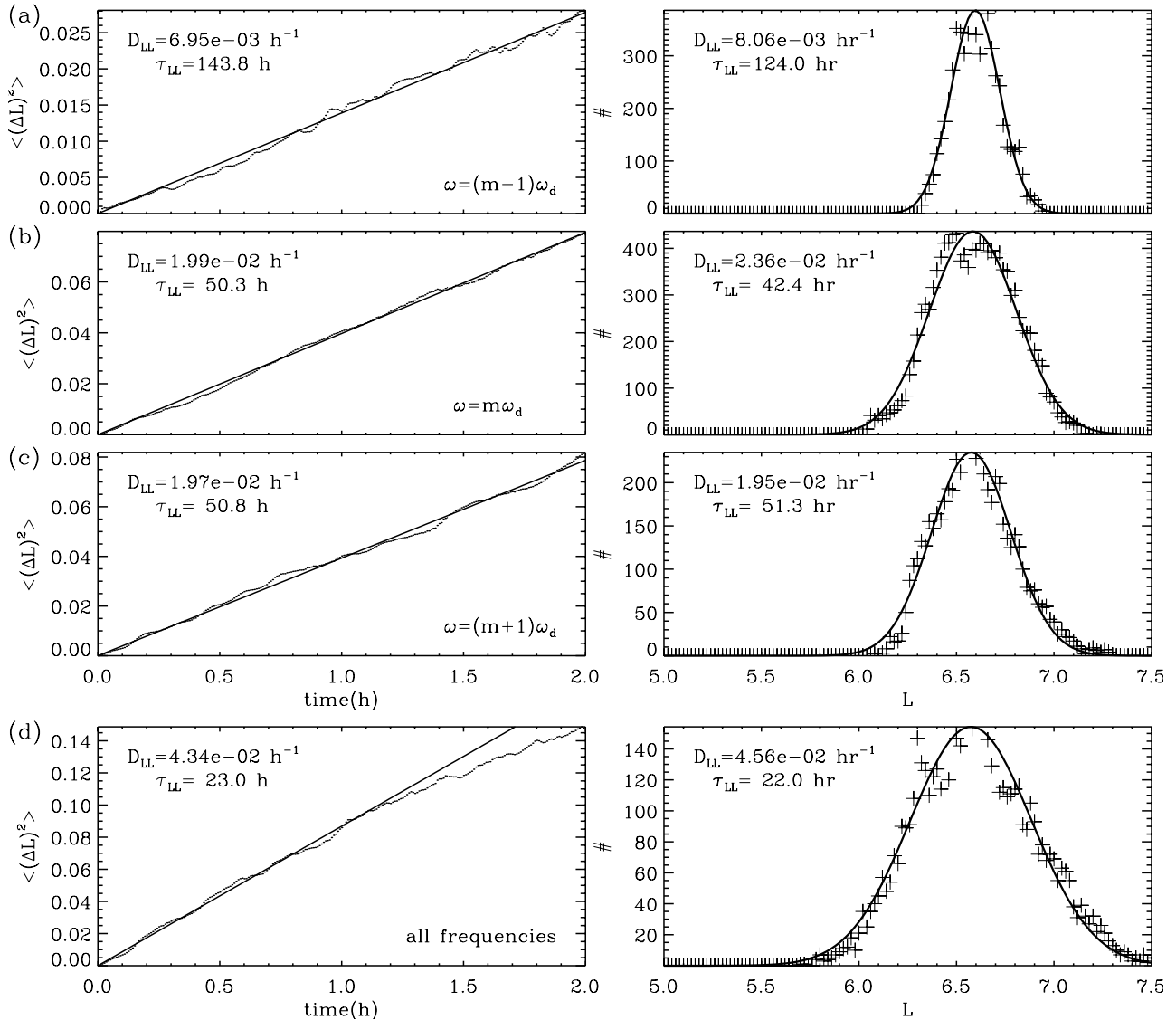


Figure 9. Mean squared spread in time (left) and particle distribution at one hour (right) for an ensemble of particles initially at $\mathcal{L} = 6.6$ and $W = 1$ MeV, in a model magnetic field corresponding to conditions during the recovery phase of the 24–26 September 1998 geomagnetic storm. Particles in panel (a) move under the influence of azimuthal $m = 2$ waves in the frequency range 0.5–2.5 mHz, exciting only the $\omega = (m - 1)\omega_d$ asymmetric resonance; those in panel (b) move under the influence of $m = 2$ waves in the frequency range 2.5–4.5 mHz, exciting only the $\omega = m\omega_d$ symmetric resonance; and particles in panel (c) move under $m = 2$, 4.7–6.7 mHz waves, exciting only the $\omega = (m + 1)\omega_d$ asymmetric resonance. Panel (d) shows the same ensemble moving under the influence of $m = 2$, 0.5–6.7 mHz waves, showing the combined effect of all three resonant modes.

of frequencies is capable of supporting each of the three resonant diffusion modes, $\omega = m\omega_d$ and $\omega = (m \pm 1)\omega_d$. As may be intuitively expected, the resulting rates of diffusion are larger than any single resonance acting alone. The calculated value, $D_{LL} \sim 4.34 \times 10^{-2} \text{ h}^{-1}$, is consistent with diffusion resulting from the simple sum of the resonances, $D_{LL} = D_{LL}^{(m-1)} + D_{LL}^{(m)} + D_{LL}^{(m+1)}$. This result suggests that, in the outer zone, power at frequencies corresponding to all three diffusive resonances must be considered in any diffusive description of the radiation belts. It is also worth noting that timescales in this case are very much in line with the shortest observed times listed in Table 1.

[43] Electrons diffuse outward faster than inward when all are initialized at the same \mathcal{L} because of the strong \mathcal{L} -dependence of the diffusion coefficient. This effect produces a narrower gaussian width on the low- \mathcal{L} side of the right panels in Figure 9, most apparent for the fastest diffusion case (d).

[44] A lower electron energy is required to satisfy the $\omega = (m + 1)\omega_d$ resonance than the $\omega = (m - 1)\omega_d$ resonance at fixed ω . Increasing the range of ω increases the range of particle energies which satisfy each resonance. At later times some electrons move inward and no longer satisfy the highest energy $(m - 1)$ resonance, while others move

outward and no longer satisfy the lowest energy ($m + 1$) resonance. This results in a decrease in the diffusion rate at later times seen in panel (d), not apparent on the two-hour timescale in the first three panels because of the smaller diffusion rate than in the combined case (d). It should also be noted that a higher wave frequency was used for the ($m + 1$) resonance in panel (c) than for the ($m - 1$) resonance in panel (a). Increasing the wave frequency decreases the time step for diffusion in a random walk process, and thus the diffusion rate increases in panel (c) relative to (a).

[45] The flat spectral profile used in generating Figure 9 may be contrasted with that leading to equation (16). In (16), the global electric field perturbation was assumed to take a specific form, namely a sharp rise in the global electric field strength followed by a slow decay (on a drift timescale), corresponding to the impulsive action of the solar wind on the magnetopause or as a result of substorm activity. Such a perturbation has a spectral profile that varies as ω_d^{-2} [Schulz and Lanzerotti, 1974]. Diffusion in this case is a result of both the intrinsic overlapping of resonances in the ω_d^{-2} profile corresponding to Figure 8 [Falthammar, 1965], as well as through the extrinsic randomness of the impulsive action (e.g., the solar wind) driving the field variations [Schulz and Lanzerotti, 1974]. In Figure 9, the extrinsic randomness of the driving perturbation present in equation (16) was simulated by running particles through a variety of wave profiles, each profile differing randomly in the initial phase of the frequency components, ξ_m . It should be noted, however, that combining both the intrinsic variability in the local fields seen by a particle (resulting from the presence of multiple waves with differing frequencies) with any extrinsic variability inherent in the driving perturbation does not serve to increase the expected rate of diffusion at a given spectral density P ; rather each effect contributes to the randomness in the guiding fields required for the particle to behave in the stochastic, diffusive manner evident in Figure 8.

[46] In a dipole field, the diffusion coefficients calculated from equation (14) are larger than those exhibited by the particular example exhibited in Figure 9 by about a factor of two. This difference can be attributed to the fact that particles drifting in a compressed dipole field will not always be drifting parallel to the azimuthal electric field as assumed in the formulation of equation (14), and will therefore gain less energy over the course of a drift orbit (equation (4)). Numerical simulations corresponding to the same frequency range and spectrum as exhibited in (Figure 9d), but in a dipole field (not shown), find $D_{LL} = 4.26 \times 10^{-2} \text{ hr}^{-1}$, very much in agreement with the analytic values expected from equation (14).

5. Conclusion

[47] We have shown that it is possible to adiabatically accelerate and transport magnetospheric electrons through a drift-resonant interaction with ULF oscillations in the Pc-5 frequency range, both individually and in bulk. The rate of energization increases with both increasing radial distortion of the magnetic field, and increasing background convection electric field. Both act to increase δr , the amplitude of drift-orbit asymmetry, which affects the range of resonant interaction with the wave as described by equation (B6). In the

case of toroidal-mode waves, with an associated radial electric field, energization occurs as a result of the electron drifting radially outward on the dawn side and radially inward on the dusk side as it interacts with the wave. With the introduction of a static convection electric field, the phase-space stability of the system is altered, allowing particles with energies below the resonant energy to be accelerated.

[48] Poloidal field line resonances, with an associated E_ϕ and small parallel magnetic disturbance in the equatorial plane, are able to efficiently accelerate single particles in a nonaxisymmetric background magnetic field, without the pitch angle scattering required for a symmetric dipole [Liu *et al.*, 1999; Summers and Ma, 2000]. In contrast to the toroidal mode, the introduction of a convection electric field to the poloidal-mode oscillations causes particles below the resonant separatrix to lose energy. This result suggests that a necessary condition for bulk electron acceleration by the single-frequency drift resonant mechanism is that there be more power in the toroidal than poloidal modes. While the most prominent waves seen in situ in AMPTE/CCE spectrograms are toroidal field line resonances [Takahashi *et al.*, 1990], analysis of CRRES magnetometer data during SSC events shows that all components are typically excited over a broader frequency range during geomagnetic storms [Miftakhova, 2001], consistent with findings by Nakamura *et al.* [2001] for the 10 March 1998 storm from Equator-S measurements.

[49] In the case of a continuum of frequencies, we find that the resonant acceleration mechanism leads to a very efficient form of radial diffusion. The results of Figure 9 suggest that diffusion rates due to ($m \pm 1$) resonant interaction with poloidal-mode fields can be at least as important as those of previous diffusion calculations, for example that represented by equation (15) and commonly used in diffusion models of the radiation belts [e.g., Brautigam and Albert, 2000; Bourdarie *et al.*, 1996; Beutier and Boscher, 1995]. Further, (Figure 9d) suggests that the various diffusion modes are additive. Diffusion calculations hoping to capture dynamic effects during periods of significant radial distortion, such as storms associated with high-speed solar wind streams and CME-magnetic cloud events, should incorporate dipole distortion effects in the model. For example, Brautigam and Albert [2000] found that radial diffusion could account for much of the variation seen in outer zone fluxes during the 9 October 1990 magnetic storm if they invoked RMS electric field amplitudes in equation (15) of up to 1.6 mV/m. Since the combined modes of diffusion discussed in this paper show greater efficiency than that of the purely symmetric $\omega = m\omega_d$ resonance alone, and since $\omega = (m \pm 1)\omega_d$ diffusion increases with both the square of the radial distortion and the square of the electric field variation, the same diffusion rates could be obtained using much more modest electric fields (and larger rates using their assumed values) by allowing for resonant diffusion effects in an asymmetric magnetic field. Furthermore, the energy dependence of equations (10) and (12) can explain greater diffusion rates at higher energies than result from equation (15), as observed [Brautigam and Albert, 2000].

[50] Further work is needed to test the functional form of the asymmetric ($m \pm 1$) diffusion against observations. A more extensive series of calculations such as seen in Figure 9, but at a variety of initial \mathcal{L} s and energies, will

verify the \mathcal{L} , W , and power variations given by equations (10) and (12); preliminary results show consistency [Eccles *et al.*, 2001]. Further analysis of the dynamics of a resonant electron in a nonaxisymmetric field may lead to more general expressions for the diffusion coefficients than those simple approximations presented in equations (10) and (12) [e.g., Brizard and Chan, 2001]. It should also be noted that many of the analytic results in this paper are model-dependent. For instance, in the equatorial plane the Mead [1964] magnetic field model exhibits a radial distortion δr that goes as r^3 [Roederer, 1970], instead of the r^4 dependence seen in equation (A4). This would lead to an asymmetric radial diffusion coefficient that varied as L^{13} , not inconsistent with the observations of Selesnick *et al.* [1997]. The equatorial plane model described here, based on a compressed dipole, appears adequate to investigate and describe the drift-resonant acceleration of electrons in an asymmetric magnetic field, as well as provide suggestions for observational evidence of such acceleration and a format to compare with other theoretical models of diffusion and acceleration.

[51] Energetic electrons in the outer zone exhibit an energy spectrum and spatial structure that can often be well-explained in terms of diffusive processes acting on trapped populations [Lyons and Thorne, 1973], but the radial diffusion rates suggested by previous calculations are too slow to account for the rapid variations often observed in outer zone electron fluxes [Walt, 1996]. Blake *et al.* [1997] showed strong correlation between solar wind dynamic pressure, IMF orientation, and energetic electron fluxes, and Li *et al.* [2001] have shown that nearly all geosynchronous variation over a 2-year period can be attributed to radial diffusion when source populations and diffusion rates were tied to solar wind speed. Work by Mann *et al.* [1999] and Mathie and Mann [2000b] suggest that during periods of high solar wind speed, enhanced ULF wave power will be seen as a result of coupling to waveguide modes in the magnetospheric cavity. During such periods, increased radial distortion of the magnetic field may be expected as a result of larger solar wind dynamic pressure acting on the magnetopause, enhancing the effect of the compressed dipole resonances (section 2) and their associated modes of radial diffusion (section 4). Observed relativistic electron flux variations on timescales of hours to ~ 1 – 2 days, occurring during storms associated with high-speed solar winds and enhanced ULF wave activity and in the presence of a suitable electron source population, may therefore be consistent with the drift-resonant acceleration processes described in this paper.

Appendix A: Particle Motion in a Compressed Dipole Magnetic Field

[52] In the absence of any perturbing forces, an equatorial electron drifting adiabatically in the geomagnetic field will move such that the guiding center drifts along contours of constant magnetic field strength. From this condition, we find that an electron drifting in a magnetic field given by equation (1) will move along a path given by

$$r(\phi) = \mathcal{L}R_E \left(1 - \frac{b_1 b_2}{B_0} \mathcal{L}^3 \cos \phi\right)^{-1/3} \quad (\text{A1})$$

where

$$\mathcal{L} = \left(\frac{R_E^3}{r_0^3} + \frac{b_1 b_2}{B_0} \cos \phi_0\right)^{-1/3} \quad (\text{A2})$$

is a parameter specifying the drift shell of an equatorial particle initially at radial distance r_0 and azimuthal angle ϕ_0 . Equation (A1) indicates that the particle will be furthest from the Earth at local noon and closest to the Earth at local midnight, as expected. The radial displacement, $\delta r = \frac{1}{2}(r_{noon} - r_{midni})$, experienced by an electron through the course of its motion can be written

$$\delta r = \frac{\mathcal{L}R_E}{2} \left[\left(1 - \frac{b_1 b_2}{B_0} \mathcal{L}^3\right)^{-1/3} - \left(1 + \frac{b_1 b_2}{B_0} \mathcal{L}^3\right)^{-1/3} \right]. \quad (\text{A3})$$

To first order in $b_1 b_2/B_0$, the radial displacement shows an \mathcal{L}^4 dependence,

$$\frac{\delta r}{R_E} \simeq \frac{b_1 b_2}{3B_0} \mathcal{L}^4, \quad (\text{A4})$$

and equation (A1) can likewise be approximately written

$$r(\phi) \simeq \mathcal{L}R_E + \delta r \cos \phi. \quad (\text{A5})$$

[53] The drift frequency of a charged particle in a compressed dipole will in general be lower than that in a pure dipole. For the magnetic field model described above, the corrected drift period can be obtained by integrating $\oint d\phi/\dot{\phi}$ over one complete drift orbit. Using $r\dot{\phi} = \frac{Mc}{\gamma e B} \frac{\partial B}{\partial r}$, we find

$$T_d = \frac{\gamma e \mathcal{L}^2 R_E^2}{3Mc} \oint \frac{1 + b_1 \mathcal{L}^3/B_0}{\left[1 - \frac{b_1 b_2}{B_0} \mathcal{L}^3 \cos \phi\right]^{5/3}} d\phi \quad (\text{A6})$$

where M is the relativistic first adiabatic invariant $p^2/2m_0B$, c is the speed of light in a vacuum, γ is the relativistic correction factor, and e is the elementary charge. The azimuthal drift velocity over the course of an orbit likewise goes as

$$v_\phi = \frac{3Mc}{\gamma e} \frac{\left(1 - \frac{b_1 b_2}{B_0} \mathcal{L}^3 \cos \phi\right)^{4/3}}{\mathcal{L}R_E \left(1 + \frac{b_1}{B_0} \mathcal{L}^3\right)}, \quad (\text{A7})$$

which, again to first order in $b_1 b_2/B_0$, can be written

$$v_\phi \simeq \bar{v} - \delta v \cos \phi \quad (\text{A8})$$

with

$$\bar{v} = \frac{3Mc}{\gamma e} \frac{1}{\mathcal{L}R_E \left(1 + \frac{b_1}{B_0} \mathcal{L}^3\right)} \quad (\text{A9})$$

$$\delta v = \frac{4Mc}{\gamma e} \frac{\frac{b_1 b_2}{B_0} \mathcal{L}^3}{\mathcal{L}R_E \left(1 + \frac{b_1}{B_0} \mathcal{L}^3\right)}. \quad (\text{A10})$$

The parameter \mathcal{L} appearing in these expressions is a third adiabatic invariant-conserving quantity, analogous to the L^*

introduced by *Roederer* [1970]. Physically, \mathcal{L} represents approximately the average radial distance (in R_E) of a particle's drift orbit, and is numerically equivalent to the radial distance of the drift path at local dawn and local dusk. We can relate \mathcal{L} to L^* using the definition $L^* = -\frac{2\pi B_0}{\Phi R_E}$ with the fields (1), where Φ is the magnetic flux contained within the particle drift orbit. The magnetic flux due to the dipole term in (1) is

$$\Phi_1 \simeq \int_{\mathcal{L}R_E}^{\infty} \int_0^{2\pi} \frac{B_0 R_E^3}{r^3} r dr d\phi = -\frac{2\pi B_0 R_E^2}{\mathcal{L}} \quad (\text{A11})$$

(see, for example, *Roederer* [1970]), while the flux due to the external terms is given by

$$\Phi_2 \simeq \int_0^{\mathcal{L}R_E} \int_0^{2\pi} (b_1 + b_1 b_2 \cos \phi) r dr d\phi = \pi b_1 \mathcal{L}^2 R_E^2. \quad (\text{A12})$$

Hence

$$L^* = \frac{\mathcal{L}}{\left(1 - \frac{b_1 \mathcal{L}^2}{2B_0}\right)}. \quad (\text{A13})$$

Generally $b_1 \ll B_0$, so $\mathcal{L} \simeq L^*$ for reasonable values of \mathcal{L} . Note that for $b_1, b_2 = 0$, both \mathcal{L} and L^* reduce to the dipole L-shell parameter *McIlwain* [1961], and equations (A6) and (A7) express the particle drift period and azimuthal drift velocity, respectively, in a pure magnetic dipole.

Appendix B: Resonant Interaction Width in Energy

[54] For the case of purely toroidal-mode waves, analytic calculations of relativistic electron interaction with the wave have been made and are similar to those given by *Chan et al.* [1989]. We begin with the relativistic expression for the change in kinetic energy given by equation (4). The fundamental toroidal mode has a magnetic node at the equator *Dungey* [1967], so for equatorial electrons $dB/dt = 0$. Assuming unperturbed azimuthal motion, $\phi = \omega_d t + \phi_0$, and radial motion of form (A5), then in the absence of a convection electric field

$$\frac{dW}{dt} = \sum_{m=0}^{\infty} \omega_d \frac{\delta \mathcal{E}_m}{2} [\cos(\Omega_{m-1} t + \xi_{m-1}) - \cos(\Omega_{m+1} t + \xi_{m+1})] \quad (\text{B1})$$

where we have defined $\delta \mathcal{E}_m = e \delta E_{rm} \delta r$, $\Omega_{m\pm 1} = (m \pm 1)\omega_d - \omega$, and $\xi_{m\pm 1} = (m \pm 1)\phi_0 + \xi_{rm}$. Integrating (B1), we find

$$W - W_0 = \sum_{m=0}^{\infty} \omega_d \frac{\delta \mathcal{E}_m}{2} \left[\frac{\sin(\Omega_{m-1} t + \xi_{m-1})}{\Omega_{m-1}} - \frac{\sin(\Omega_{m+1} t + \xi_{m+1})}{\Omega_{m+1}} \right], \quad (\text{B2})$$

from which we obtain the resonance condition equation (5). Here the “ ± 1 ” factor arises due to the $m = 1$ day-night asymmetry in the compressed dipole. Note that for $m \geq 2$ there are two possible resonances: one for $m + 1$ and one for $m - 1$. In the vicinity of one of these resonances, $\Omega_{m\pm 1} \approx 0$,

and we must first expand about the resonant energy $W = \mathcal{E}_{m\pm 1}$ before integrating (B1). There

$$\Omega_{m\pm 1} \simeq \Omega(\mathcal{E}_{m\pm 1}) + (W - \mathcal{E}_{m\pm 1}) \frac{\partial \Omega}{\partial W} \quad (\text{B3})$$

where the partial derivative is evaluated at the resonant energy $W = \mathcal{E}_{m\pm 1}$. At this energy, the first term in equation (B3) is approximately zero. The corresponding resonant term in equation (B1), with the substitution $\mathcal{Z} = \Omega_{m\pm 1} t + \xi_{m\pm 1}$, becomes

$$(W - \mathcal{E}_{m\pm 1}) dW = \omega_d \frac{\delta \mathcal{E}_m}{2} \frac{\partial \Omega}{\partial W} \cos \mathcal{Z} d\mathcal{Z} \quad (\text{B4})$$

or

$$\frac{1}{2} (W - \mathcal{E}_{m\pm 1})^2 = \omega_d \frac{\delta \mathcal{E}_m}{2} \frac{\partial \Omega}{\partial W} (\sin \mathcal{Z} - \sin \mathcal{Z}_0). \quad (\text{B5})$$

From this expression we can obtain the range in energy $W \pm \Delta \mathcal{E}_{m\pm 1}$ over which an electron experiences resonant interaction with the wave. Noting that $(\sin \mathcal{Z} - \sin \mathcal{Z}_0)$ can have a maximum value of 2, we get a half-width for the “ $m \pm 1$ ” resonance of

$$\Delta \mathcal{E}_{m\pm 1} = \sqrt{\frac{2e\delta E_{rm} \delta r}{(m \pm 1) \left[\frac{\partial(\ln \omega_d)}{\partial W} \right]_{W=\mathcal{E}_{m\pm 1}}}}. \quad (\text{B6})$$

Here the numerator represents the stronger driving effect of larger wave amplitude and of larger drift-orbit asymmetry, while the denominator shows the detuning effect of the energy dependence of the drift frequency. It should be noted that, in addition to the $\mathcal{O}[(W - \mathcal{E}_{m\pm 1})^2]$ terms truncated in (B3), (B6) is also approximate in that the effect of the “ $m \mp 1$ ” term from (B1), which, integrated, scales as $\Omega_{m\pm 1}/\Omega_{m\mp 1}$, has been ignored.

[55] **Acknowledgments.** The authors thank I. R. Mann for useful discussion and comments. Work has been supported by NSF grants ATM 98-10043 and ATM 98-19900 at LASP/SSI, NASA grants NGT5-95, NAG5-7442, and NAG5-7689 at Dartmouth College, and NSF grants ATM 96-138000 and ATM 99-01127 at Rice University. Computational work was completed with the aid of NPACI and MHPCC computers.

[56] Lou-Chang Lee and Chin S. Lin thank Danny Summers and another reviewer for their assistance in evaluating this paper.

References

- Anderson, B. J., M. J. Engebretson, S. P. Rounds, L. J. Zanetti, and T. A. Potemra, A statistical study of pulsations observed by the AMPTE/CCE magnetic fields experiment, 1, Occurrence distributions, *J. Geophys. Res.*, 95, 10,495, 1990.
- Baker, D. N., J. B. Blake, L. B. Callis, J. R. Cummings, D. Hovestadt, S. Kanekal, B. Klecker, R. A. Mewaldt, and R. D. Zwickl, Relativistic electron acceleration and decay time scales in the inner and outer radiation belts: SAMPEX, *Geophys. Res. Lett.*, 21, 409, 1994a.
- Baker, D. N., S. Kanekal, J. B. Blake, B. Klecker, and G. Rostoker, Satellite anomalies linked to electron increase in the magnetosphere, *Eos Trans. AGU*, 75, 401, 1994b.
- Baker, D. N., et al., Recurrent geomagnetic storms and relativistic electron enhancements in the outer magnetosphere: ISTP coordinated measurements, *J. Geophys. Res.*, 102, 14,141, 1997.
- Baker, D. N., J. H. Allen, S. G. Kanekal, and G. D. Reeves, Disturbed space environment may have been related to pager satellite failure, *Eos Trans. AGU*, 79, 477, 1998a.
- Baker, D. N., et al., Coronal mass ejections, magnetic clouds, and relativistic magnetospheric electron events: ISTP, *J. Geophys. Res.*, 103, 17,279, 1998b.

- Beutier, T., and D. Boscher, A three-dimensional analysis of the electron radiation belt by the Salammbô code, *J. Geophys. Res.*, *100*, 14,853, 1995.
- Birmingham, T. J., Convection electric fields and the diffusion of trapped magnetospheric radiation, *J. Geophys. Res.*, *74*, 2169, 1969.
- Blake, J. B., W. A. Kolasinski, R. W. Fillius, and E. G. Mullen, Injection of electrons and protons with energies of tens of MeV into $L < 3$ on 24 March 1991, *Geophys. Res. Lett.*, *19*, 821, 1992.
- Blake, J. B., D. N. Baker, N. Turner, K. W. Ogilvie, and R. P. Lepping, Correlation of changes in the outer-zone relativistic-electron population with upstream solar wind and magnetic field measurements, *Geophys. Res. Lett.*, *24*, 927, 1997.
- Bourdarie, S., D. Boscher, T. Beutier, J.-A. Sauvaud, and M. Blanc, Magnetic storm modeling in the Earth's electron belt by the Salammbô code, *J. Geophys. Res.*, *101*, 27,171, 1996.
- Brautigam, D. H., and J. M. Albert, Radial diffusion analysis of outer radiation belt electrons during the October 9, 1990, magnetic storm, *J. Geophys. Res.*, *105*, 291, 2000.
- Brizard, A. J., and A. A. Chan, Relativistic bounce-averaged quasilinear diffusion equation for low-frequency electromagnetic fluctuations, *Phys. Plasmas*, *8*, 4762, 2001.
- Cahill, L. J., Jr., and J. R. Winckler, Periodic magnetopause oscillations observed with the GOES satellites on March 24, 1991, *J. Geophys. Res.*, *97*, 8239, 1992.
- Chan, A. A., L. Chen, and R. B. White, Nonlinear interaction of energetic ring current protons with magnetospheric hydromagnetic waves, *Geophys. Res. Lett.*, *16*, 1133, 1989.
- Chirikov, B. V., A universal instability of many-dimensional oscillator systems, *Phys. Rep.*, *52*, 263, 1979.
- Chiu, Y. T., R. W. Nightingale, and M. A. Rinaldi, Simultaneous radial and pitch angle diffusion in the outer electron radiation belt, *J. Geophys. Res.*, *93*, 2619, 1988.
- Cornwall, J. M., Diffusion processes influenced by conjugate-point wave phenomena, *Radio Sci.*, *3*, 740, 1968.
- Dungey, J. W., Interplanetary magnetic field and the auroral zones, *Phys. Rev. Lett.*, *6*, 47, 1961.
- Dungey, J. W., Hydromagnetic waves, in *Physics of Geomagnetic Phenomena*, edited by S. Matsushita and W. H. Campbell, vol. 2, chap. V-1, p. 913, Academic, San Diego, Calif., 1967.
- Eccles, A. A., M. K. Hudson, and S. R. Elkington, A parametric study of ULF resonant-driven radial diffusion of outer zone relativistic electrons, *Eos Trans. AGU*, *82*, S354, 2001.
- Elkington, S. R., M. K. Hudson, and A. A. Chan, Acceleration of relativistic electrons via drift-resonant interaction with toroidal-mode Pc-5 ULF oscillations, *Geophys. Res. Lett.*, *26*, 3273, 1999.
- Elkington, S. R., M. K. Hudson, M. J. Wiltberger, and J. G. Lyon, MHD/particle simulations of radiation belt dynamics, *J. Atmos. Sol. Terr. Phys.*, *64*, 607, 2002.
- Engebretson, M., K.-H. Glassmeier, M. Stellmacher, W. J. Hughes, and H. Lühr, The dependence of high-latitude Pc5 wave power on solar wind velocity and on the phase of high speed solar wind streams, *J. Geophys. Res.*, *103*, 26,271, 1998.
- Fälthammar, C.-G., Effects of time-dependent electric fields on geomagnetically trapped radiation, *J. Geophys. Res.*, *70*, 2503, 1965.
- Fälthammar, C.-G., On the transport of trapped particles in the outer magnetosphere, *J. Geophys. Res.*, *71*, 1487, 1966.
- Fälthammar, C.-G., Radial diffusion by violation of the third adiabatic invariant, in *Earth's Particles and Fields*, edited by B. M. McCormac, p. 157, NATO Adv. Stud. Inst., Reinhold, New York, 1968.
- Glassmeier, K.-H., and M. Stellmacher, Concerning the local time asymmetry of Pc5 wave power at the ground and field line resonance widths, *J. Geophys. Res.*, *105*, 18,847, 2000.
- Holzworth, R. H., and F. S. Mozer, Direct evaluation of the radial diffusion coefficient near $L = 6$ due to electric field fluctuations, *J. Geophys. Res.*, *84*, 2559, 1979.
- Hudson, M. K., S. R. Elkington, J. G. Lyon, V. A. Marchenko, I. Roth, M. Temerin, J. B. Blake, M. S. Gussenhoven, and J. R. Wygant, Simulations of radiation belt formation during storm sudden commencements, *J. Geophys. Res.*, *102*, 14,087, 1997.
- Hudson, M. K., S. R. Elkington, J. G. Lyon, C. C. Goodrich, and T. J. Rosenberg, Simulation of radiation belt dynamics driven by solar wind variations, in *Sun-Earth Plasma Connections*, edited by J. L. Burch, R. L. Carovillano, and S. K. Antiochos, vol. 109, p. 171, AGU, Washington, D. C., 1999.
- Hudson, M. K., S. R. Elkington, J. G. Lyon, and C. C. Goodrich, Increase in relativistic electron flux in the inner magnetosphere: ULF wave mode structure, *Adv. Space Res.*, *25*, 2327, 2000.
- Hudson, M. K., S. R. Elkington, J. G. Lyon, M. J. Wiltberger, and M. Lessard, Radiation belt electron acceleration by ULF wave drift resonance: Simulation of 1997 and 1998 storms, in *Space Weather*, edited by P. Song, H. J. Singer, and G. L. Siscoe, vol. 125, p. 289, AGU, Washington, D. C., 2001.
- Jacobs, J. A., Y. Kato, S. Matsushita, and V. A. Troitskaya, Classification of geomagnetic micropulsations, *J. Geophys. Res.*, *69*, 180, 1964.
- Kennel, C. F., and H. E. Petschek, Limit on stably trapped particle fluxes, *J. Geophys. Res.*, *71*, 1, 1966.
- Kim, H.-J., and A. A. Chan, Fully adiabatic changes in storm-time relativistic electron fluxes, *J. Geophys. Res.*, *102*, 22,107, 1997.
- Kokubun, S., K. N. Erickson, T. A. Fritz, and R. L. McPherron, Local time asymmetry of Pc4-5 pulsations and associated particle modulations at synchronous orbit, *J. Geophys. Res.*, *94*, 6607, 1989.
- Lanzerotti, L. J., and C. G. Morgan, ULF geomagnetic power near $L = 4 - 2$, Temporal variation of the radial diffusion coefficient for relativistic electrons, *J. Geophys. Res.*, *78*, 4600, 1973.
- Lanzerotti, L. J., C. G. MacLennan, and M. Schulz, Radial diffusion of outer-zone electrons: An empirical approach to third-invariant violation, *J. Geophys. Res.*, *75*, 5351, 1970.
- Li, X., I. Roth, M. Temerin, J. R. Wygant, M. K. Hudson, and J. B. Blake, Simulation of the prompt energization and transport of radiation belt particles during the March 24, 1991 SSC, *Geophys. Res. Lett.*, *20*, 2423, 1993.
- Li, X., D. N. Baker, M. Temerin, D. Larson, R. P. Lin, G. D. Reeves, M. Looper, S. G. Kanekal, and R. A. Mewaldt, Are energetic electrons in the solar wind the source of the outer radiation belt?, *Geophys. Res. Lett.*, *24*, 923, 1997.
- Li, X., D. N. Baker, M. Temerin, G. D. Reeves, and R. D. Belian, Simulation of dispersionless injections and drift echoes of energetic electrons associated with substorms, *Geophys. Res. Lett.*, *25*, 3763, 1998.
- Li, X., M. Temerin, D. N. Baker, G. D. Reeves, and D. Larson, Quantitative prediction of radiation belt electrons at geostationary orbit based on solar wind measurements, *Geophys. Res. Lett.*, *28*, 1887, 2001.
- Lichtenberg, A. J., and M. A. Lieberman, *Applied Mathematical Sciences*, 2nd ed., vol. 38, *Regular and Chaotic Dynamics*, Springer-Verlag, New York, 1983.
- Liu, W. W., G. Rostoker, and D. N. Baker, Internal acceleration of relativistic electrons by large-amplitude ULF pulsations, *J. Geophys. Res.*, *104*, 17,391, 1999.
- Lyons, L. R., and M. Schulz, Access of energetic particles to storm time ring current through enhanced radial "diffusion", *J. Geophys. Res.*, *94*, 5491, 1989.
- Lyons, L. R., and R. M. Thorne, Equilibrium structure of radiation belt electrons, *J. Geophys. Res.*, *78*, 2142, 1973.
- Lysak, R. L., and D. Lee, Response of the dipole magnetosphere to pressure pulses, *Geophys. Res. Lett.*, *19*, 937, 1992.
- Mann, I. R., A. N. Wright, K. J. Mills, and V. M. Nakariakov, Excitation of magnetospheric waveguide modes by magnetosheath flows, *J. Geophys. Res.*, *104*, 333, 1999.
- Mathie, R. A., and I. R. Mann, A correlation between extended intervals of ULF wave power and storm-time geosynchronous relativistic electron flux enhancements, *Geophys. Res. Lett.*, *27*, 3261, 2000a.
- Mathie, R. A., and I. R. Mann, Observations of Pc5 field line resonance azimuthal phase speeds: A diagnostic of their excitation mechanism, *J. Geophys. Res.*, *105*, 10,713, 2000b.
- McAdams, K. L., and G. D. Reeves, Non-adiabatic response of relativistic radiation belt electrons to GEM magnetic storms, *Geophys. Res. Lett.*, *28*, 1879, 2001.
- McIlwain, C. E., Coordinates for mapping the distribution of magnetically trapped particles, *J. Geophys. Res.*, *66*, 3681, 1961.
- Mead, G. D., Deformation of the geomagnetic field by the solar wind, *J. Geophys. Res.*, *69*, 1181, 1964.
- Miftakhova, E., A study of Pc5 ULF oscillations, Master's thesis, Dartmouth College, Hanover, NH, 2001.
- Nakamura, R., J. B. Blake, S. R. Elkington, D. N. Baker, and W. Baumjohann, Relationship between ULF waves and radiation belt electrons during the March 10, 1998 storm, *Adv. Space Res.*, *30*(10), 2163, 2002.
- Newkirk, L. L., and M. Walt, Radial diffusion coefficient for electrons at low L values, *J. Geophys. Res.*, *73*, 1013, 1968a.
- Newkirk, L. L., and M. Walt, Radial diffusion coefficient for electrons at $1.76 < L < 5$, *J. Geophys. Res.*, *73*, 7231, 1968b.
- Nishida, A., and K. Maezawa, Two basic modes of interaction between the solar wind and the magnetosphere, *J. Geophys. Res.*, *76*, 2254, 1971.
- Northrop, T. G., *The Adiabatic Motion of Charged Particles*, Wiley-Interscience, New York, 1963.
- O'Brien, T. P., R. L. McPherron, D. Sornette, G. D. Reeves, R. Friedel, and H. J. Singer, Which magnetic storms produce relativistic electrons at geosynchronous orbit?, *J. Geophys. Res.*, *106*, 15,533, 2001.
- Paulikas, G. A., and J. B. Blake, Effects of the solar wind on magnetospheric dynamics: Energetic electrons at the synchronous orbit, in *Quantitative Modeling of Magnetospheric Processes*, vol. 21, edited by W. P. Olsen, p. 180, AGU, Washington, D. C., 1979.

- Perreault, P., and S.-I. Akasofu, A study of geomagnetic storms, *Geophys. J. R. Astron. Soc.*, *54*, 547, 1978.
- Ridley, A. J., G. Lu, C. R. Clauer, and V. O. Papitashvili, Ionospheric convection during nonsteady interplanetary magnetic field conditions, *J. Geophys. Res.*, *102*, 14,563, 1997.
- Ridley, A. J., G. Lu, C. R. Clauer, and V. O. Papitashvili, A statistical study of the ionospheric convection response to changing interplanetary magnetic field conditions using the assimilative mapping of ionospheric electrodynamics technique, *J. Geophys. Res.*, *103*, 4023, 1998.
- Riley, P., and R. A. Wolf, Comparison of diffusion and particle drift descriptions of radial transport in the Earth's inner magnetosphere, *J. Geophys. Res.*, *97*, 16,865, 1992.
- Roederer, J. G., *Dynamics of Geomagnetically Trapped Radiation*, Springer-Verlag, New York, 1970.
- Rostoker, G., S. Skone, and D. N. Baker, On the origin of relativistic electrons in the magnetosphere associated with some geomagnetic storms, *Geophys. Res. Lett.*, *25*, 3701, 1998.
- Ruohoniemi, J. M., and R. A. Greenwald, The response of high-latitude convection to a sudden southward IMF turning, *Geophys. Res. Lett.*, *25*, 2913, 1998.
- Ruohoniemi, J. M., R. A. Greenwald, K. B. Baker, and J. C. Samson, HF radar observations of Pc 5 field line resonances in the midnight/early morning MLT sector, *J. Geophys. Res.*, *96*, 15,697, 1991.
- Saunders, M. A., M. P. Freeman, D. J. Southwood, S. W. H. Cowley, M. Lockwood, J. C. Samson, C. J. Farrugia, and T. J. Hughes, Dayside ionospheric convection changes in response to long-period interplanetary magnetic field oscillations: Determination of the ionospheric phase velocity, *J. Geophys. Res.*, *97*, 19,373, 1992.
- Schulz, M., and A. Eviatar, Diffusion of equatorial particles in the outer radiation zone, *J. Geophys. Res.*, *74*, 2182, 1969.
- Schulz, M., and L. J. Lanzerotti, *Physics and Chemistry in Space*, vol. 7, *Particle Diffusion in the Radiation Belts*, Springer-Verlag, New York, 1974.
- Selesnick, R. S., and J. B. Blake, On the source location of radiation belt relativistic electrons, *J. Geophys. Res.*, *105*, 2607, 2000.
- Selesnick, R. S., J. B. Blake, W. A. Kolasinski, and T. A. Fritz, A quiescent state of 3 to 8 MeV radiation belt electrons, *Geophys. Res. Lett.*, *24*, 1343, 1997.
- Summers, D., and C.-Y. Ma, Rapid acceleration of electrons in the magnetosphere by fast-mode MHD waves, *J. Geophys. Res.*, *105*, 15,887, 2000.
- Takahashi, K., B. J. Anderson, and R. J. Strangeway, AMPTE CCE observations of Pc 3–4 pulsations at $L = 2-6$, *J. Geophys. Res.*, *95*, 17,179, 1990.
- Tomassian, A. D., T. A. Farley, and A. L. Vampola, Inner-zone energetic electron repopulation by radial diffusion, *J. Geophys. Res.*, *77*, 3441, 1972.
- Tsyganenko, N. A., and D. P. Stern, Modeling the global magnetic field of the large-scale Birkeland current systems, *J. Geophys. Res.*, *101*, 27,187, 1996.
- Walt, M., Source and loss processes for radiation belt particles, in *Radiation Belts: Models and Standards*, vol. 97, edited by J. F. Lemaire, D. Heynderickx, and D. N. Baker, p. 1, AGU, Washington, D. C., 1996.
- Wrenn, G. L., Conclusive evidence for internal dielectric charging anomalies on geosynchronous communications spacecraft, *J. Spacecr. Rockets*, *32*, 514, 1995.

A. A. Chan, Department of Physics and Astronomy, Rice University, Houston, TX 77005, USA.

S. R. Elkington, Laboratory for Atmospheric and Space Physics, University of Colorado, Boulder, CO 80303, USA. (scot.elkington@lasp.colorado.edu)

M. K. Hudson, Department of Physics and Astronomy, Dartmouth College, Hanover, NH 03755, USA.